Journal of Science and Technology
on Information and Communications

Calibration of Gain Mismatches in TIADCs using Convolutional Neural Networks

Ta Van Thanh[1], Quach Ngoc Tang[2], and Le Nhat Thang[3]

[1]Faculty of Radio Communication, Telecommunications University, Khanh Hoa, Vietnam
[2]Technical College of Communications, Hanoi, Vietnam
[3]Posts and Telecommunications Institute of Technology, Hanoi, Vietnam

CORRESPONDING AUTHOR: Le Nhat Thang (e-mail: thangln@ptit.edu.vn).

Received 22 December, 2025; revised 11 May, 2026; accepted 12 May, 2026; Date of publication 20 May, 2026; date of current version 20 May, 2026.

Digital Object Identifier 10.66890/JSTIC.2026.11.01.101

ABSTRACT Time-interleaved analog-to-digital converters (TIADCs) are widely used in high-speed sampling systems, but their performance is degraded by channel mismatches among sub-ADCs. This paper presents a lightweight one-dimensional convolutional neural network (1-D CNN)-based calibration method for compensating gain mismatches in TIADCs. The proposed CNN is trained in a supervised manner to estimate the gain-mismatch-induced error component from the distorted TIADC output. During training, the target error is generated from the difference between the gain-mismatched TIADC output and a reference mismatch-free ADC output. During inference, only the TIADC output is required, and the calibrated signal is reconstructed by subtracting the estimated error from the mismatched output. Simulation results for 4-channel and 8-channel TIADC systems show that the proposed method effectively suppresses gain-mismatch-induced spurious tones. For the 4-channel TIADC, the proposed calibration improves SNDR by 31.23 dB and SFDR by 61.44 dB. For the 8-channel TIADC, improvements of 32.43 dB in SNDR and 61.02 dB in SFDR are achieved. The proposed CNN contains approximately 17k trainable parameters, suggesting its potential for low-complexity digital background calibration.

INDEX TERMS TIADC, channel mismatch, gain mismatch, calibration, convolutional neural network.

I. INTRODUCTION

In modern broadband communication and high-speed data acquisition systems, signal digitization is required to achieve increasingly higher sampling rates and accuracy. Time-interleaved analog-to-digital converters (TIADCs) have emerged as a promising solution to meet these demands [1], [2]. The key advantage of the TIADC architecture is its ability to increase the overall sampling rate without degrading the resolution or accuracy of the conversion. A TIADC employs multiple sub-ADCs operating in parallel and sampling the input signal in a time-staggered manner. Each channel samples the input at distinct instants, and their outputs are multiplexed to form the composite high-rate output. Ideally, an M-channel TIADC achieves an M-fold increase in sampling rate, where M is the number of interleaved channels [2].

While TIADCs offer high sampling efficiency with power and accuracy comparable to single-channel ADCs, their performance is strongly affected by mismatches among sub-ADCs. In practice, TIADC systems typically suffer from three major mismatch types: offset, gain, and timing mismatches [2]–[6]. Among them, gain mismatch is particularly detrimental, as it introduces spurious tones at frequencies $f_s/2 \pm f_{in}$, severely degrading TIADC performance. Therefore, accurate estimation and compensation of gain mismatch are essential to improving TIADC output quality. Existing calibration approaches can be broadly classified into foreground and background techniques [7]. Although foreground calibration delivers high accuracy, it requires interruption of normal TIADC operation and the use of dedicated calibration signals, making it unsuitable for real-time communication systems. Background calibration overcomes this limitation by operating continuously without halting the converter, but it typically involves substantial computational complexity and slow convergence, which pose challenges for hardware implementation [4]–[8]. These limitations create opportunities for machine-learning-based calibration, as neural networks can learn mismatch behaviors directly from data without relying on analytical mismatch models. Recent studies have demonstrated the potential of such approaches for TIADC calibration [9], [10].

Numerous studies have proposed traditional calibration techniques for gain mismatches in TIADCs. Several methods employ digital filtering, modulation matrices, Hadamard transforms, and optimization algorithms (e.g., LS, LMS) to estimate and correct offset, gain, and timing mismatches simultaneously [3]–[5], [7], [11]. In particular, gain mismatch is commonly compensated by estimating the inter-channel energy ratio or by using bandpass filtering techniques [5], [12]. However, these methods often suffer from limitations in accuracy, convergence speed, or computational complexity, especially as the number of channels increases or at high operating frequencies. Recently, convolutional neural networks (CNNs) have emerged as a promising approach to address these challenges due to their strong capability in handling nonlinear relationships and automatically extracting features from signal data. In addition, neural-network-based calibration has attracted increasing attention for ADC and TIADC systems. Peng et al. proposed a neural-network-based calibration technique for TI-ADCs using derivative information [13]. Lu et al. further introduced an ANN-based calibration mechanism for ADCs and demonstrated its effectiveness using a time-interleaved ADC case study [14]. More recent works have explored fast-convergence NN-based background calibration for timing mismatch, CNN-based timing-skew calibration, and machine-learning-based blind digital calibration for TIADCs [15]–[19]. These studies demonstrate the potential of data-driven approaches for improving TIADC performance. However, most existing neural-network-based TIADC calibration studies focus on timing skew or general mismatch correction, whereas the present work specifically investigates a lightweight 1-D CNN residual-error estimation framework for gain-mismatch calibration.

Motivated by these advantages, this paper investigates the characteristics of gain mismatch in TIADCs and proposes a CNN-based method for gain-mismatch estimation and compensation. The proposed calibration model leverages a CNN to extract gain-mismatch features from the TIADC output by comparing them with reference TIADC data and isolating the corresponding mismatch components. These estimated gain mismatches are then subtracted from the TIADC output. The effectiveness of the proposed technique is validated through simulation results.

The main contributions of this paper are summarized as follows. First, a lightweight one-dimensional CNN-based residual-error estimation framework is proposed for gain-mismatch calibration in TIADCs. Unlike approaches that directly estimate correction coefficients or reconstruct the corrected signal without explicitly defining the error target, the proposed method formulates the CNN output as the gain-mismatch-induced error component. Second, the training and inference procedures are clearly separated: the reference ADC output is used only during supervised offline training to generate error labels, whereas online calibration requires only the mismatched TIADC output and a forward pass of the trained CNN. Third, the proposed architecture uses a compact 1-D CNN with kernel sizes of 7, 5, and 3 samples, making it suitable for signal-frame-based calibration. Finally, the effectiveness of the method is verified on both 4-channel and 8-channel TIADC systems, and the computational complexity of the proposed network is analyzed in terms of trainable parameters and MAC operations.

The rest of the paper is organized as follows. Section II presents the system model while Section III presents the mathematical model of TIADC and the proposed calibration method. In Section IV, the paper conducts verification simulations, analyzes the results obtained. Finally, the conclusion of the paper is presented in Section V.

II. SYSTEM MODEL

Consider a TIADC model that includes only gain mismatch while assuming all other mismatch components are absent. This model is illustrated in Fig. 1. The analog input signal $x(t)$ is a band-limited sinusoidal signal sampled by each sub-ADC channel at the frequency f_s/M. In this case, the output signal of the i-th channel can be expressed as follows

$$y_i[k] = g_i x[kM + i] \tag{1}$$

Therefore, the time-domain output of the i-th channel can be expressed as follows

$$\begin{aligned} y_i(t) &= \sum_{k=-\infty}^{k=+\infty} y_i[k]\delta(t - (kM + i)T_s) \\ &= \sum_{k=-\infty}^{k=+\infty} g_i x[(kM + i)T_s]\delta(t - (kM + i)T_s) \end{aligned} \tag{2}$$

After multiplexing, the time-domain output $y(t)$ of the TIADC can be expressed as follows

$$\begin{aligned} y(t) &= \sum_{i=0}^{M-1} y_i(t) \\ &= \sum_{i=0}^{M-1} \sum_{k=-\infty}^{k=+\infty} g_i x[(kM+i)T_s]\delta(t-(kM+i)T_s) \end{aligned} \quad (3)$$

In this expression, $y_i(t)$ is the output of the i-th sub-ADC, g_i denotes the gain mismatch of channel i-th, and M is the number of interleaved channels (with $i = 0, ..., M-1$). By performing a frequency-domain analysis for a sinusoidal input signal with frequency ω_{in}, the output spectrum of the TIADC with gain mismatch only can be expressed as follows

$$\begin{aligned} Y(j\omega) = \frac{1}{T_s} \sum_{k=-\infty}^{+\infty} \underbrace{\left[\frac{1}{M} \sum_{i=0}^{M-1} g_i . e^{-jki\frac{2\pi}{M}} \right]}_{\text{Gainmismatch}} \\ \times X\left(j\left(\omega - k\frac{\omega_s}{M} \right) \right). \end{aligned} \quad (4)$$

Equation (4) shows that the gain mismatch is a function of the number of interleaved channels M, and that the gain values g_i of each channel do not depend on the input frequency ω_{in}. The additional components caused by the modulation effect of the input signal produce spectral replicas of the input. As a result, the output spectrum exhibits spurious tones at frequencies $\pm\omega_{in} + k\frac{\omega_s}{M}$, that is, at $\pm f_{in} + k\frac{f_s}{M}$. From a frequency-domain perspective, it can be observed that the locations of the gain-mismatch-induced spurs depend on the input signal frequency.

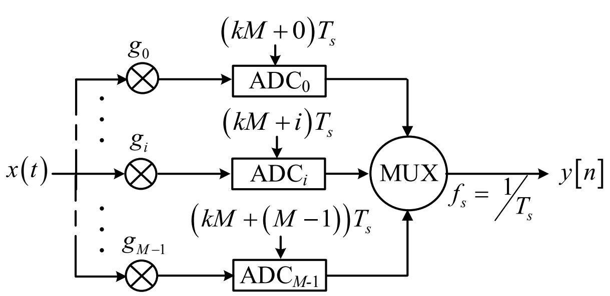

FIGURE 1. TIADC model with gain mismatch only.

III. PROPOSED CALIBRATION TECHNIQUE

Convolutional neural networks (CNNs), a subclass of artificial neural networks (ANNs), were originally developed and primarily used for visual image analysis. They represent an enhanced form of multilayer perceptrons specifically designed to process grid-structured data such as images and time-series signals. In recent years, the rapid advancement of CNN applications in digital signal processing has opened a new research direction. CNNs have demonstrated outstanding capabilities in handling nonlinear signals and decomposing them into characteristic frequency components within the signal-processing domain. A notable advantage is that many CNN architectures can operate directly on raw input data without requiring any additional preprocessing, thereby simplifying the data preparation stage.

CNNs offer strong abilities in capturing temporal information, automatically extracting features from data, scaling effectively to large datasets, and exhibiting high flexibility for various signal-processing tasks. These characteristics are particularly important when dealing with nonlinear and nonstationary signals in real-time applications. Motivated by these advantages, this paper proposes a background-calibration approach that applies CNNs to compensate for gain mismatches in TIADCs.

The proposed model employs a one-dimensional CNN architecture for gain-mismatch calibration, as illustrated in Fig. 2. It incorporates two separate input branches to achieve accurate mismatch estimation:

- TIADC output with gain mismatch: This is the primary data stream from the practical TIADC system, containing distortions caused by gain mismatch. It is fed into the CNN so that the network can extract mismatch-related features.

- Reference ADC output: This is an ideal mismatch-free signal obtained from a continuously operating reference ADC. During training, this signal serves as the ground truth. The CNN learns to compare the distorted TIADC output with the ideal reference signal to accurately estimate the gain mismatch.

To avoid ambiguity, the proposed CNN is designed as a residual-error estimator for gain-mismatch calibration. Specifically, the CNN estimates the gain-mismatch-induced error component rather than directly producing the corrected signal or channel correction coefficients. During training, the target label is defined as the difference between the mismatched TIADC output and the reference ADC output. During inference, the trained CNN predicts the gain-mismatch error component from the mismatched TIADC output only. The calibrated output is then obtained by subtracting the estimated error from the original TIADC output.

The proposed CNN operates in two distinct phases, namely the training phase and the inference (online calibration) phase:

Training phase: During training, the CNN receives both the mismatched TIADC output and the reference ADC output. The objective is to learn a complex mapping that enables accurate estimation of the gain mismatch by contrasting the two signals. A mean squared error (MSE) loss function is used to minimize the difference between the estimated and actual mismatch values (derived from the discrepancy between the mismatched and reference outputs).

Inference (online calibration) phase: After training, the CNN takes only the mismatched TIADC output and predicts the estimated gain mismatch. This estimated mismatch is then subtracted from the TIADC output to obtain the calibrated signal.

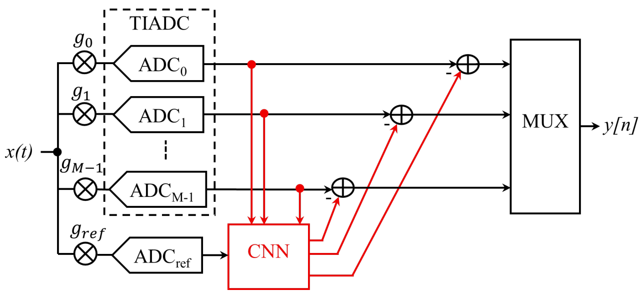

FIGURE 2. Block diagram of the proposed gain-mismatch calibration model

The proposed CNN-based calibration model is structured as follows:

- **Input:** During training, the mismatched TIADC output is used as the network input, while the reference ADC output is used to generate the supervised error label. During inference, only the mismatched TIADC output is used as the input to the trained CNN. Each input frame is formed from D consecutive samples of the multiplexed TIADC output sequence $y[n]$. Since the TIADC output is obtained by interleaving M sub-ADC channels, one frame may equivalently contain L consecutive samples from each sub-ADC channel, where $D = M \times L$. In the proposed 1-D CNN framework, however, the input frame is arranged as a one-dimensional sequence of length D before being applied to the network. Here, M denotes the number of interleaved channels, L denotes the number of samples per channel within one frame, and D denotes the total frame length. During training, the corresponding reference ADC sequence $x_{\text{ref}}[n]$ with the same length D is used only to generate the supervised error label $e[n] = y[n] - x_{\text{ref}}[n]$. During inference, only the mismatched TIADC output frame $y[n]$ is required. In this work, a reference ADC operating continuously at sampling frequency f_s is used to generate the labels for the network.

- **CNN Architecture:** The proposed CNN architecture is illustrated in Fig. 3. It begins with three consecutive 1-D convolutional layers, each configured with an appropriate number of kernels and kernel sizes. The three convolutional layers use 32, 64, and 32 filters with 1-D kernel sizes of 7, 5, and 3 samples, respectively. The padding values are set to 3, 2, and 1 to preserve the temporal dimension of the feature maps. The final 1-D convolution layer uses one filter with kernel size 1 to map the extracted features into the estimated gain-mismatch-induced error sequence. A ReLU activation function follows each convolution layer to introduce nonlinearity. Each convolution layer produces a set of feature maps that serve as the input to the next layer in the sequence.

Finally, a fully connected (FC) operation is employed to aggregate the extracted features and reconstruct the gain-mismatch values, which are then subtracted from the TIADC output. In the proposed CNN architecture (shown in Fig. 3), the FC function is implemented implicitly in the final layer through a 1 convolution operation. Although not explicitly labeled as a "fully connected layer," this 1 convolution performs the same functional role by linearly combining the feature maps from the previous stage and compressing them from 32 channels into a single output channel. This serves as the final transformation step of the network, converting the extracted mismatch-related features into a corrected signal that is subsequently subtracted from the TIADC output.

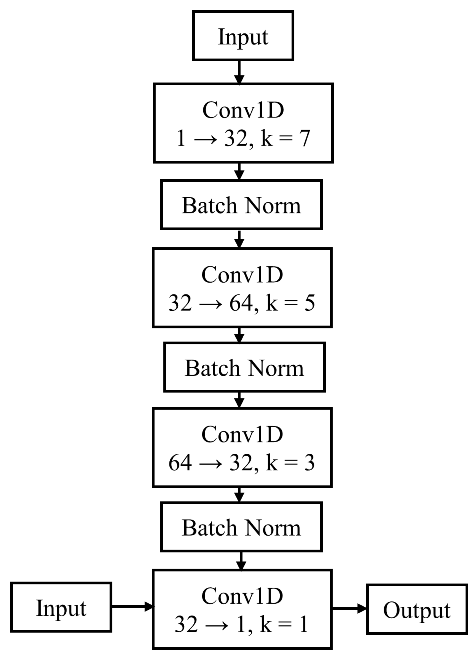

FIGURE 3. Proposed 1-D CNN architecture for gain-mismatch-induced error estimation.

The output of the network is the estimated gain-mismatch-induced error sequence $\hat{e}[n]$, which has the same length as the input frame. The calibrated output is obtained as

$$\hat{x}[n] = y[n] - \hat{e}[n], \tag{5}$$

where $y[n]$ denotes the mismatched TIADC output and $\hat{x}[n]$ denotes the calibrated digital output.

- **Loss function:** The MSE loss function is calculated between the estimated error $\hat{e}[n]$ and the target error

$e[n]$, where

$$e[n] = y[n] - x_{\text{ref}}[n], \tag{6}$$

where $x_{\text{ref}}[n]$ is reference signal during training (ideal ADC output). Therefore, the loss function is defined as

$$L_{\text{MSE}} = \frac{1}{N} \sum_{n=1}^{N} \left(\hat{e}[n] - e[n]\right)^2, \tag{7}$$

where N denotes the number of samples used to compute the loss. In this work, N corresponds to the number of samples in an input frame; when mini-batch training is used, the loss is averaged over all samples in the mini-batch.

- **Training:** Training samples are obtained from the reference ADC together with the gain-mismatched outputs of the practical ADC channels. All data are normalized to a common scale. The network is trained in a supervised manner using the reference ADC samples as the ground-truth labels for each channel. After training, the calibration process only requires forward inference, enabling online gain-mismatch correction.

IV. NUMERICAL RESULTS AND DISCUSSION

To evaluate the effectiveness of the proposed technique, simulations are conducted on 4-channel and 8-channel TIADC systems operating at a sampling rate of 2.7 GSPS, with a single-tone sinusoidal input signal at $f_{in} = 0.45 f_s$. The dataset was generated using sinusoidal input signals sampled by the simulated TIADC model. The gain mismatch of each sub-ADC channel was randomly drawn from a uniform distribution within $\pm 3\%$. Each data frame consisted of L consecutive samples from each of the M interleaved channels. After multiplexing, each frame was arranged as a one-dimensional input sequence with length $D = M \times L$. The target label was defined as the gain-mismatch-induced error sequence

$$e[n] = y[n] - x_{\text{ref}}[n], \tag{8}$$

where $y[n]$ is the gain-mismatched TIADC output and $x_{\text{ref}}[n]$ is the corresponding reference ADC output. The dataset was divided into training, validation, and test subsets with a ratio of 70%/15%/15%. All signals were normalized to a common amplitude range before training. The CNN model parameters are configured as described in Section III. The training dataset is generated from sampled signals. The model inputs consist of the gain-mismatched TIADC output signal (in 1D form) and the output of a reference ADC.

The CNN architecture comprises three consecutive 1-D convolutional layers. The first convolutional layer employs 32 filters with a kernel size of 7 samples to extract low-level and general features from the input signal. Padding is set to 3 to prevent rapid reduction of the output dimensionality. The output of this layer is fed into a batch normalization block to normalize the convolution outputs, thereby accelerating training and stabilizing gradient propagation. The second convolutional layer consists of 64 filters with a kernel size of 5 samples, enabling the extraction of more complex features, particularly capturing spatiotemporal variations in the ADC signals. A subsequent batch normalization layer further improves convergence and mitigates vanishing or exploding gradient issues. The ReLU activation function and batch normalization are interleaved within the network to enhance nonlinear feature learning and improve feature discrimination capability. The third convolutional layer employs 32 filters with a kernel size of 3 samples, reducing the feature depth to 32 channels while emphasizing the most relevant learned features.

The CNN output stage compresses the feature representation from 32 channels into a single output channel using a 1-D convolution with kernel size 1, which performs a linear combination of the extracted features without altering the spatial dimensions. The loss function is defined as the MSE between the estimated gain-mismatch-induced error and the target error sequence defined in (6). The calibrated signal is then reconstructed by subtracting the estimated error from the mismatched TIADC output. The objective is to minimize this squared error. The proposed CNN model is trained in a supervised manner using the prepared dataset. After training, the calibration process requires only forward inference, enabling real-time operation.

During training, the number of epochs is set to 500, the batch size is 500 samples, and the Adam optimizer is employed with an initial learning rate of 0.001, which is reduced every 100 epochs using a learning-rate scheduler. The calibrated output signal can be directly compared with the ground truth or used as input for spectral reconstruction to evaluate performance metrics such as the signal-to-noise-and-distortion ratio (SNDR) and the spurious-free dynamic range (SFDR).

The computational complexity of the proposed CNN is also estimated. For a 1-D convolutional layer, the number of trainable parameters is calculated as

$$P_l = C_{\text{out},l} \left(C_{\text{in},l} K_l + 1\right), \tag{9}$$

where $C_{\text{in},l}$, $C_{\text{out},l}$, and K_l denote the number of input channels, output channels, and kernel size of the l-th layer, respectively. Based on the proposed architecture, the parameter counts of the four convolutional layers are $32(1 \times 7 + 1) = 256$, $64(32 \times 5 + 1) = 10{,}304$, $32(64 \times 3 + 1) = 6{,}176$, and $1(32 \times 1 + 1) = 33$, respectively. Thus, the convolutional layers contain 16,769 trainable parameters. The batch-normalization layers add $2(32 + 64 + 32) = 256$ trainable scale and shift parameters. Therefore, the proposed CNN contains approximately 17,025 trainable parameters, i.e., about 17k parameters.

The number of multiply–accumulate operations (MACs) per output sample is estimated from the convolutional operations as

$$32\times1\times7+64\times32\times5+32\times64\times3+1\times32\times1 = 16{,}640. \quad (10)$$

Therefore, the proposed CNN requires approximately 16.6k MACs per output sample, excluding bias additions, activation functions, and batch-normalization overhead. These values indicate that the proposed network is lightweight. Nevertheless, measured inference latency and hardware resource utilization are not evaluated in this work.

After simulation, the convergence of the calibrated signal toward the desired reference signal is illustrated in Fig. 4. As shown in Fig. 4, the corrected signal (solid green line) closely follows the ideal reference signal (blue dashed line). Fig. 4 shows the calibrated output obtained during the inference phase after the CNN has been trained offline. Therefore, the overlap between the calibrated signal and the reference signal should not be interpreted as instantaneous training convergence. In this work, the CNN is trained offline for 500 epochs with a batch size of 500. After training, online calibration only requires a forward pass of the trained network to estimate the gain-mismatch-induced error component. Since measured inference latency and hardware resource utilization are not evaluated in this work, no numerical latency value is reported. Therefore, the proposed method is described as having potential for low-latency background calibration rather than as a fully demonstrated real-time implementation.

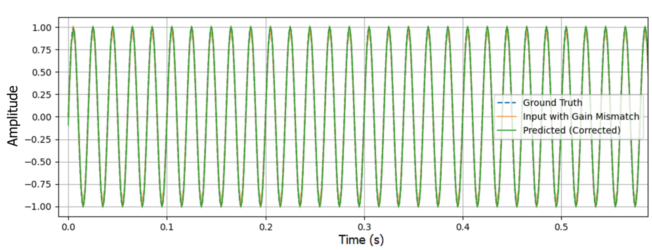

FIGURE 4. The convergence of the signal after correction.

To evaluate the performance of the TIADC after applying the proposed CNN-based calibration model, simulations are conducted to analyze the power spectral density (PSD) of the TIADC output signals before and after calibration. The simulation results for 4-channel and 8-channel TIADC systems are illustrated in Fig. 5 and Fig. 6, respectively. The results demonstrate that the spurious components caused by gain mismatches are significantly suppressed, leading to improved TIADC performance.

The TIADC performance before and after calibration is quantitatively evaluated using the signal-to-noise-and-distortion ratio (SNDR) and the spurious-free dynamic range (SFDR). The proposed model achieves substantial performance improvements. Specifically, for the 4-channel TIADC, the SNDR is improved by 31.23 dB (from 29.51 dB to 60.74 dB), while the SFDR is improved by 61.44 dB (from 32.72 dB to 94.16 dB). Similarly, for the 8-channel TIADC, performance gains of 32.43 dB in SNDR and 61.02 dB in SFDR are obtained. These results confirm that the proposed calibration model effectively compensates for gain mismatches in TIADCs with different numbers of interleaved channels.

To further clarify the position of the proposed method with respect to existing TIADC calibration techniques, Table 1 provides a qualitative comparison between the proposed CNN-based approach and representative traditional and neural-network-based calibration methods. The comparison highlights the calibration target, calibration type, main technique, convergence process, and implementation complexity reported or implied in previous studies.

It should be noted that a strictly fair numerical comparison under identical simulation conditions is difficult because the prior studies use different TIADC resolutions, sampling frequencies, input-frequency ranges, mismatch assumptions, and evaluation metrics. Therefore, Table I provides a methodological and performance-oriented comparison based on the reported characteristics of representative calibration methods. Compared with traditional adaptive or analytical calibration techniques, the proposed method avoids iterative mismatch-coefficient adaptation during the online calibration stage. Compared with recent neural-network-based methods, the proposed approach focuses on a lightweight 1-D CNN residual-error estimator for gain-mismatch-induced error compensation, requiring only the mismatched TIADC output during inference.

Since the simulation settings of previous studies are different, a strictly fair numerical comparison based only on published results is difficult. Therefore, an additional same-setup baseline experiment is conducted using a conventional channel-gain normalization method, as reported in Table 2.

For a more direct comparison under the same simulation conditions, a conventional channel-gain normalization method is also implemented as a traditional baseline. Since only gain mismatch is considered in this work, the baseline estimates the relative gain of each sub-ADC channel from its RMS value as in [3]–[6], [20]. Let $y_i[k]$ denote the output sequence of the i-th sub-ADC channel. The estimated channel amplitude is calculated as

$$A_i = \sqrt{\frac{1}{K}\sum_{k=1}^{K} y_i^2[k]}, \quad (11)$$

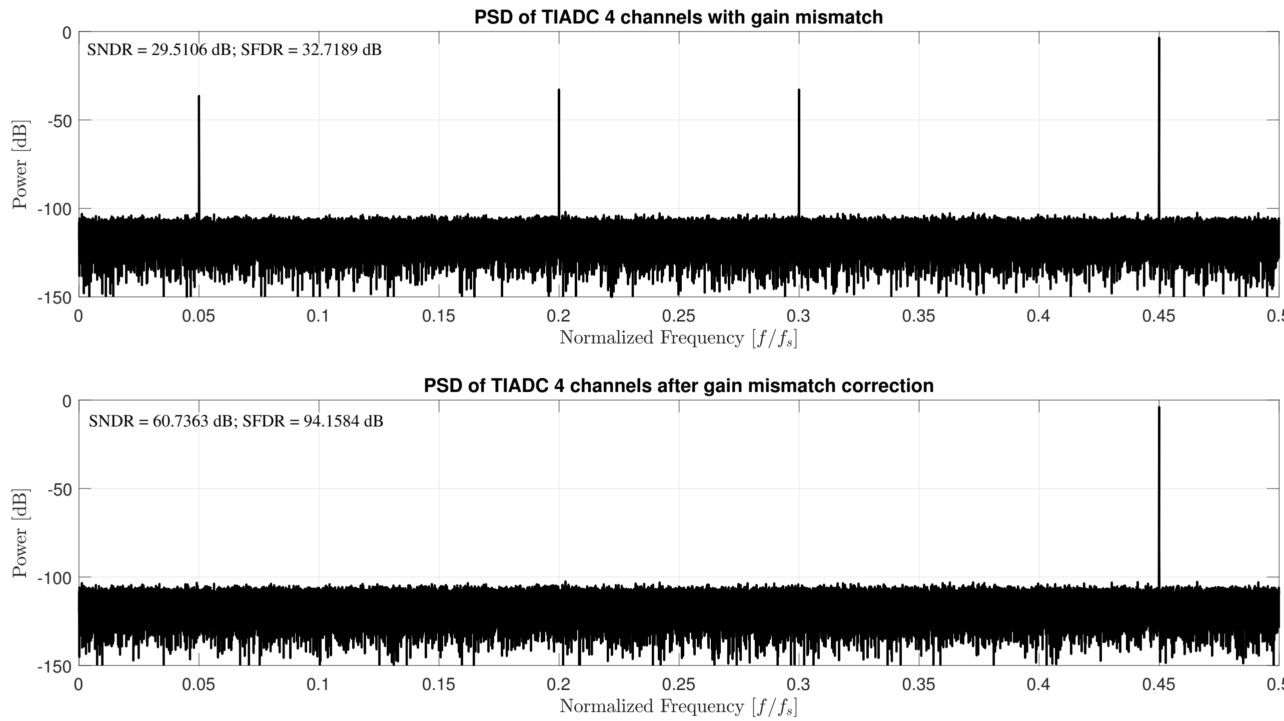

FIGURE 5. The output frequency spectrum of the 4-channel TIADC before and after calibration.

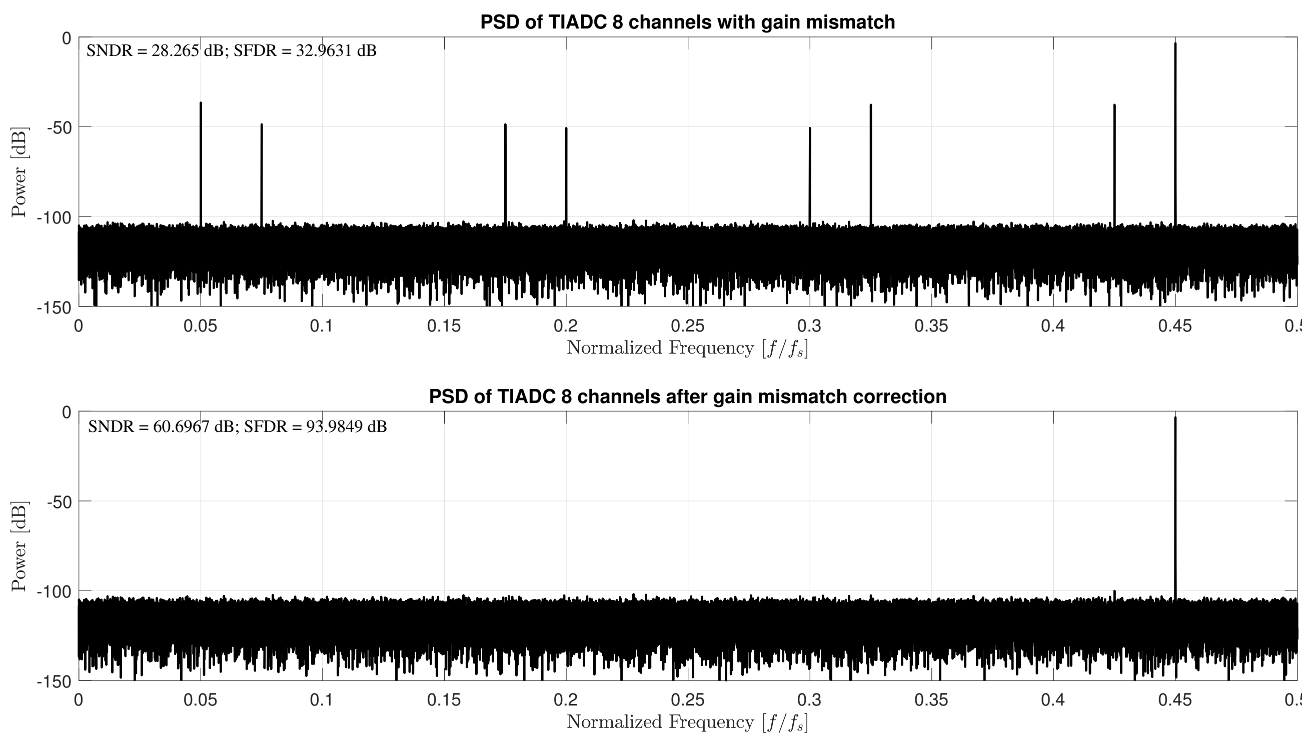

FIGURE 6. The output frequency spectrum of the 8-channel TIADC before and after calibration.

where K is the number of samples used for gain estimation in each channel. The average channel amplitude is then obtained as

$$\bar{A} = \frac{1}{M} \sum_{i=0}^{M-1} A_i. \tag{12}$$

TABLE 1. Qualitative comparison with representative TIADC calibration methods

Method	Calibration target	Type	Main technique	Performance / convergence / complexity	Remarks
Ta et al. [3]	Offset, gain, and timing mismatches	Background	All-digital calibration	SNDR/SFDR results are not directly comparable under the same setup; iterative/adaptive digital calibration; analytical digital processing.	Traditional calibration method.
Ta et al. [4]	Channel mismatches	Background	Improved all-digital calibration	SNDR/SFDR results are not directly comparable under the same setup; iterative background calibration; analytical mismatch processing.	Requires explicit mismatch model.
Le et al. [7]	Gain and timing mismatches	Background	Adaptive noise canceller	SNDR/SFDR results are not directly comparable under the same setup; adaptive-filtering convergence; filter-based complexity.	LMS/ANC-based calibration method.
Lu et al. [9]	ADC/TIADC mismatch	NN-based	ANN-based calibration	Different simulation/hardware setting; offline training and inference; NN complexity is not directly comparable.	Closely related NN-based approach.
Peng et al. [10]	TIADC mismatch	NN-based	NN with derivative information	Different simulation setting; offline training and inference; requires derivative-information processing.	Related NN-based method.
Proposed	Gain mismatch	CNN-based	Lightweight 1-D CNN residual-error estimator	SNDR: +31.23 dB / +32.43 dB; SFDR: +61.44 dB / +61.02 dB; offline training with 500 epochs; online calibration by one forward pass; ≈17k parameters and ≈16.6k MACs/sample.	Only mismatched TIADC output is required during inference.

TABLE 2. Same-setup quantitative comparison with a conventional gain-normalization baseline

TIADC	Method	SNDR (dB)	SFDR (dB)	Notes
4-channel	Uncalibrated	29.51	32.72	No calibration
4-channel	Gain-normalization baseline	60.69	93.56	Same setup
4-channel	Proposed CNN	60.74	94.16	Same setup
8-channel	Uncalibrated	28.27	32.96	No calibration
8-channel	Gain-normalization baseline	60.67	93.69	Same setup
8-channel	Proposed CNN	60.70	93.98	Same setup

The normalized output of the i-th channel is given by

$$\tilde{y}_i[k] = \frac{\bar{A}}{A_i} y_i[k]. \tag{13}$$

Finally, the corrected sub-ADC outputs are multiplexed to reconstruct the calibrated TIADC output. This baseline is evaluated using the same 4-channel and 8-channel TIADC simulation settings as the proposed CNN-based method.

As shown in Table 2, the conventional gain-normalization baseline improves the SNDR and SFDR compared with the uncalibrated TIADC output. However, the proposed CNN-based method achieves higher performance under the same simulation conditions. This indicates that the proposed residual-error estimation framework can suppress gain-mismatch-induced spurious components more effectively than simple channel-gain normalization.

Fig. 7 illustrates the SNDR performance of the TIADC as a function of the normalized input frequency f/f_s before and after applying the proposed gain-mismatch calibration method. Prior to calibration, the SNDR exhibits a pronounced degradation as the input frequency increases. This degradation is mainly caused by spurious spectral components generated by gain mismatches among the interleaved sub-ADCs. The effect becomes more severe at mid-to-high input frequencies, where mismatch-induced harmonics significantly deteriorate the TIADC performance.

After applying the proposed CNN-based calibration, a substantial improvement in SNDR is observed across

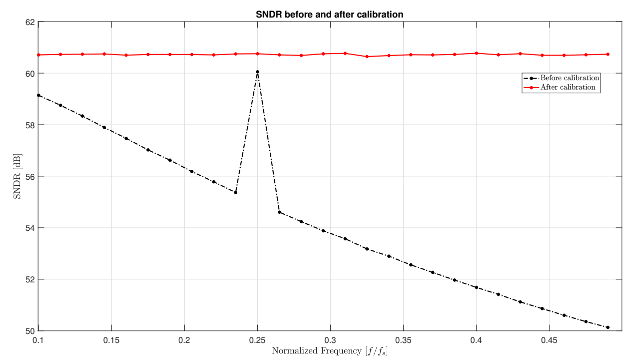

FIGURE 7. SNDR before and after calibration.

the entire evaluated frequency range. The calibrated SNDR remains nearly constant at approximately 60–61 dB, demonstrating a high degree of robustness with respect to variations in the input signal frequency. This behavior indicates that the proposed method effectively suppresses gain-mismatch-induced spurs and restores the output signal quality of the TIADC.

A direct comparison between the calibrated and uncalibrated cases shows that the SNDR improvement increases with the input frequency, reaching its maximum in the high-frequency region, where gain mismatch has the most detrimental impact. These results confirm the strong generalization capability of the proposed CNN-based calibration method for different input frequencies and its independence from specific signal conditions.

Overall, the simulation results demonstrate that the proposed gain-mismatch calibration approach significantly enhances the TIADC performance while maintaining stable SNDR over a wide frequency range. This makes the proposed method particularly suitable for broadband and high-speed TIADC applications that require consistent performance under varying input signal conditions.

V. CONCLUSIONS

This paper presented a lightweight 1-D CNN-based method for gain-mismatch calibration in TIADCs. The proposed CNN was formulated as a residual-error estimator that learns the gain-mismatch-induced error component from the distorted TIADC output. During supervised training, the error label was obtained from the difference between the mismatched TIADC output and the reference ADC output. After training, the calibrated signal was reconstructed by subtracting the CNN-estimated error from the TIADC output. Simulation results demonstrated that the proposed method effectively suppresses gain-mismatch-induced spurious tones and significantly improves SNDR and SFDR for both 4-channel and 8-channel TIADC systems. The calibrated SNDR remained stable over the evaluated input-frequency range, indicating the robustness of the proposed method under different signal conditions. The proposed CNN has a lightweight architecture with approximately 17k trainable parameters, suggesting its potential for low-complexity digital background calibration. However, hardware implementation, measured inference latency, power consumption, and FPGA/ASIC resource utilization were not investigated in this work. Future research will focus on hardware implementation, online adaptive learning, and extension of the proposed framework to jointly compensate offset, gain, and timing mismatches in TIADCs.

REFERENCES

[1] W. C. Black and D. A. Hodges, "Time interleaved converter arrays," *IEEE J. Solid-State Circuits*, vol. 15, no. 6, pp. 1022–1029, 1980.

[2] N. Kurosawa, H. Kobayashi, K. Maruyama, H. Sugawara, and K. Kobayashi, "Explicit analysis of channel mismatch effects in time-interleaved ADC systems," *IEEE Trans. Circuits Syst. I Fundam. Theory Appl.*, vol. 48, no. 3, pp. 261–271, 2002.

[3] V.-T. Ta, V.-P. Hoang, and X. N. Tran, "All-Digital Background Calibration Technique for Offset, Gain and Timing Mismatches in Time-Interleaved ADCs," *EAI Endorsed Trans. Ind. Networks Intell. Syst.*, vol. 6, no. 21, pp. e3, 2019.

[4] V.-T. Ta, V.-P. Hoang, V.-P. Pham, and C.-K. Pham, "An improved all-digital background calibration technique for channel mismatches in high speed time-interleaved analog-to-digital converters," *Electronics*, vol. 9, no. 1, p. 73, 2020.

[5] V.-T. Ta and V.-P. Hoang, "Combined Power Ratio Calculation, Hadamard Transform and Least Mean Squares Algorithm for Channel Mismatch Calibration in Time-Interleaved ADCs," *VNU J. Sci.: Comput. Sci. Commun. Eng.*, vol. 36, no. 2, 2020.

[6] V.-P. Hoang and V.-T. Ta, "Fully digital background calibration of channel mismatches in time-interleaved ADCs using recursive least square algorithm," *AEU-Int. J. Electron. Commun.*, vol. 130, p. 153574, 2021.

[7] D. H. Le, T. K. P. Dinh, V.-P. Hoang, and D. M. Nguyen, "All-digital background calibration of gain and timing mismatches in time-interleaved ADCs using adaptive noise canceller," *AEU-Int. J. Electron. Commun.*, vol. 114, p. 152999, 2020.

[8] J. Sung and J. Choi, "A New Interpretation of the Time-Interleaved ADC Mismatch Problem: A Tracking-Based Hybrid Calibration Approach," arXiv preprint arXiv:2503.10022, 2025.

[9] Z. Lu, B. Zhang, X. Peng, H. Liu, X. Ye, Y. Li, Y. Peng, Y. Xiao, W. Zhang, and H. Tang, "A new artificial neural network-based calibration mechanism for ADCs: a time-interleaved ADC case study," *IEEE Trans. Very Large Scale Integr. (VLSI) Syst.*, vol. 32, no. 7, pp. 1184–1194, 2024.

[10] X. Peng, X. Ye, H. Liu, Z. Lu, Y. Xiao, Y. Peng, and H. Tang, "A neural network based calibration technique for TI-ADCs with derivative information," in *Proc. IEEE Int. Symp. Circuits Syst. (ISCAS)*, 2023, pp. 1–5.

[11] L. Guo, S. Tian, and Z. Wang, "Estimation and correction of gain mismatch and timing error in time-interleaved ADCs based on DFT," *Metrol. Meas. Syst.*, vol. 21, no. 3, pp. 535–544, 2014.

[12] J. Matsuno, T. Yamaji, M. Furuta, and T. Itakura, "All-digital background calibration technique for time-interleaved ADC using pseudo aliasing signal," *IEEE Trans. Circuits Syst. I Reg. Papers*, vol. 60, no. 5, pp. 1113–1121, 2013.

[13] X. Peng, X. Ye, H. Liu, Z. Lu, Y. Xiao, Y. Peng, and H. Tang, "A Neural Network Based Calibration Technique for TI-ADCs with Derivative Information," in *Proc. IEEE Int. Symp. Circuits Syst. (ISCAS)*, 2023, pp. 1–5, doi: 10.1109/ISCAS46773.2023.10181825.

[14] Z. Lu, B. Zhang, X. Peng, H. Liu, X. Ye, Y. Li, Y. Peng, Y. Xiao, W. Zhang, and H. Tang, "A New Artificial Neural Network-Based Calibration Mechanism for ADCs: A Time-Interleaved ADC Case Study," *IEEE Trans. Very Large Scale Integr. (VLSI) Syst.*, vol. 32, no. 7, pp. 1184–1194, 2024, doi: 10.1109/TVLSI.2024.3390220.

[15] Z. Lu, B. Zhang, Y. Peng, X. Peng, H. Tang, J. Pu, L. Qin, and M. Guo, "A Novel NN-Based Fast-Convergence Background Calibration for Timing Mismatch in TI ADCs," *IEEE Trans. Circuits Syst. II, Exp. Briefs*, vol. 72, no. 1, pp. 48–52, 2025, doi: 10.1109/TCSII.2024.3477463.

[16] D. Li, T. Yang, L. Wang, S. Lang, H. Liang, and Z. Zhu, "FR-CNN: Frequency Recognition Convolutional Neural Network-Based Calibration for Timing Skew in TI-ADCs," *IEEE Trans. Circuits Syst. II, Exp. Briefs*, vol. 72, no. 12, pp. 1957–1961, 2025, doi: 10.1109/TCSII.2025.3630996.

[17] T. Li, Y. Zhou, N. Dang, D. Fang, P. Chen, X. Fu, D. Xu, M. Gong, J. Jiang, and J. Zhang, "A TI-ADC Calibration Method Based on Structured Pruning Neural Network with Multi-Tone Signal Pre-Training," *Microelectron. J.*, vol. 172, Art. no. 107144, 2026, doi: 10.1016/j.mejo.2026.107144.

[18] S. P. Bhanushali, S. Nasrin, D. Maiti, and A. Sanyal, "Machine-learning Based Blind Digital Calibration of Time-Interleaved ADC," in *Proc. IEEE 43rd VLSI Test Symp. (VTS)*, 2025, doi: 10.1109/VTS65138.2025.11022918.

[19] M. Chen, Y. Zhao, N. Xu, F. Ye, and J. Ren, "A Partially Binarized and Fixed Neural Network Based Calibrator for SAR-Pipelined ADCs Achieving 95.0-dB SFDR," in *Proc. IEEE Int. Symp. Circuits Syst. (ISCAS)*, 2021, pp. 1–4, doi: 10.1109/ISCAS51556.2021.9401089.

[20] V.-T. Ta, "Research on calibration method of channel mismatches in time-interleaved ADC," *Le Quy Don Technical University*, 2021.

Ta Van Thanh received a B.Eng. degree in Telecommunication technological command from the Military Communication Officers' Training College (Vietnam) in 2010. He obtained Master Degree in Telecommunication Engineering from the Post and Telecommunications Institute of Technology (Vietnam) in 2014, and the Ph.D. degree in Electronic Engineering at Le Quy Don Technical University (LQDTU) in 2022. His research interests include digital systems, signal processing, wireless communications systems, high-speed hardware implementation, AI... Currently, he is a lecturer at the

Faculty of Radio Communication, Telecommunications University (TCU), Khanh Hoa, Vietnam.

Quach Ngoc Tang received the B.Eng. degree in Electrical and Electronic Engineering from the Military Technical Academy, Vietnam, in 2008. He is currently pursuing the M.Sc. degree in Telecommunications Engineering at the Posts and Telecommunications Institute of Technology. His research interests include electronic engineering, telecommunications electronics, wireless communications systems, and artificial intelligence. He is currently the Head of the Department of Electronic Warfare Engineering at the Technical College of Communications (TCC), Vietnam.

Le Nhat Thang received the B.Eng degree in Radio - Electronics and Communication from Hanoi University of Science and Technology (HUST), Vietnam, in 1995, the M.Eng degree in Telecommunications from the Asian Institute of Technology (AIT), Bangkok, Thailand, in 2000 and Ph.D. degree in Information and Communication Technology (ICT) from the Department of Computer Science and Telecommunications (DIT), University of Trento, Italy in 2006. He is currently an Associate Professor, the Dean of the Vietnam Institute of Leadership, Governance and Management (VLGM), and the Secretary of the Doctoral Council at the Posts and Telecommunications Institute of Technology (PTIT), Hanoi, Vietnam, after having served for more than 10 years as the Dean of the Postgraduate Studies Faculty. His research interests include performance analysis, modeling and simulation, wireless communication systems, physical layer security, queueing theory and its applications, machine learning, deep learning, optimization, and biomedical applications.